Materials Research. 2018; 21(4): e20180138
DOI: http://dx.doi.org/10.1590/1980-5373-MR-2018-0138

HVOF-sprayed Coating Over AISI 4140 Steel for Hard Chromium Replacement

***Anael Preman Krelling*[a]*, *Matheus Machado de Souza*[b], *Cesar Edil da Costa*[b], *Julio César Giubilei Milan*[b]**

[a]*Instituto Federal de Santa Catarina - IFSC, Rua Pavão, 1377, CEP 89220-618, Joinville, SC, Brasil*
[b]*Universidade do Estado de Santa Catarina - UDESC, Avelino Marcante Bairro Zona Industrial Norte, s/n, CEP 89219710, Joinville, SC, Brasil*

Received: February 22, 2018; Revised: April 16, 2018; Accepted: April 20, 2018

The replacement of electrolytic hard chrome (EHC) by high velocity oxy-fuel (HVOF) sprayed coatings is investigated due to the toxicity of EHC process. The wear behavior of AISI 4140 steel coated by HVOF-, EHC-process was compared to quenched and tempered (Q&T) steel using a pin-on-disc apparatus. The wear tests were conducted at room temperature, 10 N applied load and 0.1 m/s sliding speed in dry condition. The results were interpreted on the basis of the microstructure and hardness. Wear micromechanisms were investigated by SEM. The predominant presence of the WC phase and the formation of W_2C and W_3C phases, associated with decarburization of superheated regions of the CoCr binding phase of HVOF-coated samples were observed by X-ray diffraction analysis. Wear tests results show that the WC-10Co-4Cr coating exhibits better wear resistance than the EHC coating and Q&T steel. The formation of a wear resistant tribolayer was determinant to the excellent wear behavior of the thermally sprayed coating.

Keywords: *thermal spray coating, HVOF, tribological behavior, sliding wear, wear micromechanism.*

1. Introduction

Many components associated with the energy generation industry, use surface coating as an alternative to complete replacement of mechanical elements in processes that are usually associated with maintenance shutdowns and production losses. AISI 4140 steel is universally accepted in the steel, automotive, power generation and oil extraction industries, as it is present in gears, pipe joints, rolling rolls, turbines, electric generators and drive systems.

Hard chromium coating electroplated[1] or electrolytic hard chrome (EHC)[2] is one of the most used surface treatment applied to ensure surface wear and corrosion resistance[3]. However, chromium is on the list of toxic materials according to Environmental Protection Agency (EPA)[4]. The acid bath generated by the electrolytic process contains high amounts of Cr^{6+} ions that are dispersed through the air and are difficult to trap in filters and drains[2,5]. Current environmental legislation restricts the use of chemicals containing hexavalent chromium ions and grounds the need to develop alternative coating processes less harmful to the environment[4].

In addition to the environmental problems, technically, in the EHC are some negative aspects such as the hydrogen embrittlement and the non-guarantee of the quality and homogeneity of the treatment[6,7]. The presence of micro-cracks and tensile stresses in the coating-substrate interface contribute to the delamination of the chromium layer and reduction of the material's fatigue resistance[3,8,9].

The replacement of EHC by thermally sprayed wear-resistant coatings is widely studied in the literature[1,2,7,10,11]. A wide range of materials can be processed by plasma, flame and electric arc spraying in applications ranging from gas turbine technology to the electronics industry[1]. All of them have been able to replace the traditional chrome plating process, in particular the HVOF (high velocity oxy-fuel)[8] which produces highly adherent coatings, with low porosity (< 1%) and good corrosion resistance[10,12].

Papers of HVOF-sprayed coatings of commercial composition (WC-10Co-4Cr) have been published in a number of journals. This is the most popular composition of HVOF-sprayed coatings[13]. Most of these papers investigated its microstructure, corrosion and tribological properties, and also used as-sprayed or polished surfaces that have high and low roughness values, respectively[12,14-17].

Hong et al.[14] employed the Taguchi method to optimize the HVOF spray parameters. Samples of sprayed WC-10Co-4Cr coating were polished by 2.5 and 0.5 µm diamond pastes prior to pin-on-disc sliding tests. An Al_2O_3 polished ball was used as counter-body with an applied load of 70 N, 1500 m sliding distance and sliding velocity of 0.9 m/s without lubrication at room temperature. Coated samples exhibit better wear resistance than Cr12MoV cold work die steel. Wear process occurred by the extrusion of Co-Cr matrix followed by the crack and removal of WC particles.

*anael.krelling@ifsc.edu.br

Polished HVOF-sprayed coatings of WC-10Co-4Cr was analyzed by Bolelli et al.[13] and Wu et al.[15] under dry sliding conditions. Ra roughness values lower than 0.12 µm were obtained after polishing process. At room temperature extrusion deformation and abrasive wear mechanism takes place at 10 N[13] and 30-50 N[15]. At 750 °C WC-10Co-4Cr experiences catastrophic oxidation[13].

Erosion wear experiments were carried out on as-sprayed WC-10Co-4Cr coating by Singh et al.[12]. The authors found a roughness of 4.24 µm for coated SS304 steel. WC-10Co-4Cr coating provides better wear resistance than Ni-20Cr_2O_3 coating. The roughness values of as-sprayed coatings, however, are higher than the acceptable limits for many industrial applications[18].

WC-10Co-4Cr as-sprayed coating was sanded up to 220 grit in SiC abrasive paper by Federici et al.[19] to achieve a surface roughness to about 1 µm prior to the wear tests. The authors carried out pin-on-disc sliding tests of coated and uncoated cast iron at room temperature and 300 °C with a nominal contact pressure of 1 MPa at 1.57 m/s for 50 min after a running in step of 10 min. Commercial brake pads pins (6 mm in diameter) were used as counter-body. Due to a friction layer formation at 300 °C the friction coefficient remains constant since the beginning of the tests and the wear rates of HVOF-sprayed coatings were negligible.

Therefore, the aim of this work is to evaluate the microstructure and the tribological behavior of AISI 4140 steel coated by HVOF-, EHC-process and also the Quenched and Tempered (Q&T) steel. After the HVOF- and EHC-process samples were grinded to achieve roughness values below 1 µm (Ra). We believe that this condition is industrially more favorable than polished or as-sprayed coatings.

2. Experimental Procedure

The chemical composition of the AISI 4140 steel used in this work is given in Table 1. A bar with 50.8 mm of diameter was cut into 10 mm thick samples.

All samples were quenched and tempered (Q&T) before coating application. The samples were austenitized at 890 °C and oil quenched. Tempering treatment was performed at 200 °C for 2 h followed by heating at 580 °C for more 2 h.

After the Q&T treatment the samples were grinded in the faces intended for coating deposition. Prior to the coating processes the average roughness value was 3.17 µm.

2.1. Sample characterization

The microstructure and morphology of the coatings were evaluated by optical and electronic microscopy. Samples were cut in cross-section in a Buehler Isomet 4000 with 2650 rpm and 1.2 mm/min feed rate, sanded up to 600 grit in SiC abrasive paper, polished with 1 µm alumina suspension and etched with 3% Nital solution.

Vickers microhardness tests were carried out in a Shimadzu HMV-2T tester with 100 g ($HV_{0.1}$) applied load and dwell time of 10 seconds. At least 5 indentations were made on each position for determination of the hardness profile.

Phase identification was made by X-ray diffraction (XRD) analysis in a Shimadzu PW1800 difractometer with copper tube and Mo Kα (1.54060 A) radiation over a 2θ range of 10-100°. A step size of 0.02° with 1 second scan step time was used. X'Pert HighScore from PANalytical was used to the phase identification.

2.2. Electrolytic hard chrome deposition

The preparation of the samples included the plastic painting in the faces which the hard chrome was not deposited. Samples were cleaned with alkaline degreaser and anodic etched of 20 A/dm² for 1-3 minutes.

The electroplating was carried out in a 3000 A and 380 V Eiko current rectifier at Cromagem Jaraguá. The bath composition was CrO_3 230 g/l + H_2SO_4 1.2 g/l, bath temperature of 58-62 °C, current density of 40 A/dm² and deposition rate of 20-25 µm/h for 8.5 h. The de-hydrogenation thermal treatment (190 °C for 6 h) was performed for all samples.

The roughness obtained after the electroplating treatment deposition was 0.68 ± 0.17 µm (Ra) and 4.28 ± 0.69 µm (Rz). Ra is defined as the average absolute deviation of the roughness irregularities from the mean line, while Rz is the difference in height between the average of the five highest peaks and the five lowest valleys along the assessment length of the profile[20].

2.3. Thermal spraying treatment (HVOF)

HVOF-spray runs were performed with a Praxair-Tafa HP-HVOF JP5000 (barrel length of 152 mm) at Rijeza Metalurgia. WC-10Co-4Cr (WOKA 3652, -45 +15µm, spherical, agglomerated and sintered), thermal spray powder was employed. Spraying distance was maintained in 305 mm. The other spraying parameters are listed in Table 2.

The roughness obtained after the thermal spraying treatment was 2.96 ± 0.11 µm (Ra) and 15.75 ± 0.36 µm (Rz).

2.4. Tribological behavior

Pin-on-disc wear tests were carried out according to ASTM G99 standard. Before the test the samples were grinded to a Ra roughness about 1 µm and cleaned with acetone. Five tests were performed for each sample condition. The counter-body was a polished alumina ball with 6 mm diameter. The wear test were carried out with the following

Table 1. Chemical composition of AISI 4140 steel used in this work (wt-%).

C	S	Mn	Si	P	Cr	Mo
0.38-0.43	0.04 (max.)	0.75-1.00	0.15-0,35	0.03 (max.)	0.80-1.10	0.15-0.25

Table 2. HVOF spraying parameters.

Parameter	WC-10Co-4Cr	Unit
Aspersion rate	90	g/min
Kerosene flux	23	l/min
O_2 flux	875	l/min
Kerosene pressure	11.5 ± 1	bar
O_2 pressure	10 ± 0.3	bar
Combustion pressure	7 ± 0.3	bar

parameters: room temperature (25 °C), 10 N applied load, 0.1 m/s sliding speed, 1000 m sliding distance and 6 mm of wear track radius. The wear track profile was measured in a Mitutoyo Contrace CV2000 profilometer in order to determine the average transverse area (6 profiles) of the wear track. The volume of material removed (VMR) was calculated by a multiplication of the average wear track area by the track length 2πR, where R is the wear track radius. Wear micromechanisms were investigated by SEM.

3. Results and Discussion

3.1. Microstructure

Figure 1 shows the XRD patterns for Electroplated (Hard Chromium) and Thermally Sprayed (WC-10Co-4Cr) AISI 4140 steel. For the chromium coating, it was not possible to verify the peaks attributed to metallic chromium and chromium oxide, probably existing on the surface of the coating. Although the EDS (Figure 2) technique indicated the presence of oxygen in the coating, the thin surface of chromium oxide was not detected under the conditions used in X-ray diffraction, as discussed in[20].

For HVOF coated specimens the predominant presence of the WC phase was observed[21]. For the curve between the angles of 30° and 50° in 2θ (Figure 1) a cobalt and chromium binding phase of amorphous or nanocrystalline nature is attributed[19,22,23]. This amorphous phase is often found in this type of coating because of its high cooling rate[22,24]. The formation of W_2C and W_3C phases is associated with decarburization of superheated regions of the CoCr binding phase[14]. WC precipitation occurs only if the temperature of any region of a heated particle is above the melting temperature of the WC-10Co-4Cr eutectic ternary and is usually related to the decarburization of these regions[25]. After the impact of these particles, W_2C and W_3C phases precipitate from the supersaturated binder phase, forming smaller layers to the environments of the existing WC particles[22,25].

Figure 3 shows the presence of cracks and microcracks in an amorphous structure in the region coated with hard chromium in a similar manner to what happens in other works[20,26]. In the coating-substrate interface it is possible to

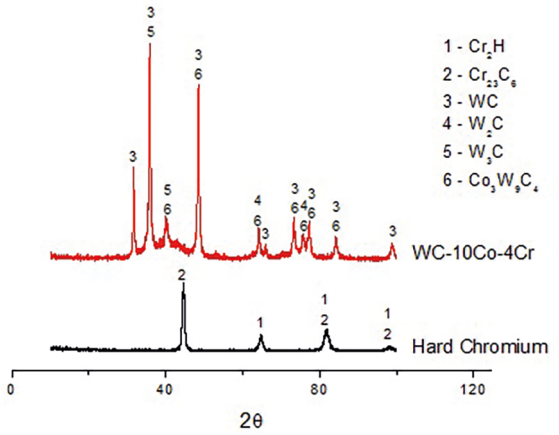

Figure 1. X-ray diffraction patterns of electroplated (Hard Chromium) and thermally sprayed (WC-10Co-4Cr) AISI 4140 steel.

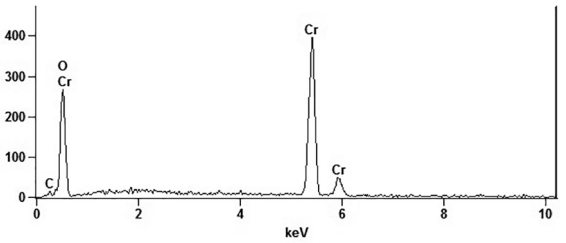

Figure 2. EDS analysis on the surface of the electroplated AISI 4140 steel.

note the presence of faults in the coating adhesion caused by oxide incrustations. Oxidized particles are an element that affects the thermal and mechanical behavior around the region in which they are present. Besides that it can be a stress raiser element and modify the deformation behavior of the material[28]. Residual tensile stresses are common characteristics found in hard chromium coatings from the decomposition of chromium hydrides during the electrodeposition process. This decomposition is accompanied by a reduction of volume (up to 15%) favoring the appearance of residual tensile stresses in the substrate immediately below the coating, resulting in the formation of microcracks[4]. The hard chromium coating thickness obtained before the grinding process was 203 ± 16 µm.

The HVOF coatings showed dense lamellar structure involved by oxide films, low porosity and low quantities of oxide films in the coating-substrate interface[27]. In Figure 4 the light gray represents the tungsten carbides and the darker phase indicates the CoCr amorphous matrix as identified by X-ray diffraction analysis[22,28]. The WC-10Co-4Cr coating thickness obtained before the grinding process was 281 ± 23 µm.

For the microhardness profile curve of each coating, ten measuring points were considered as shown in Figure 5. The average microhardness value is indicated for each region.

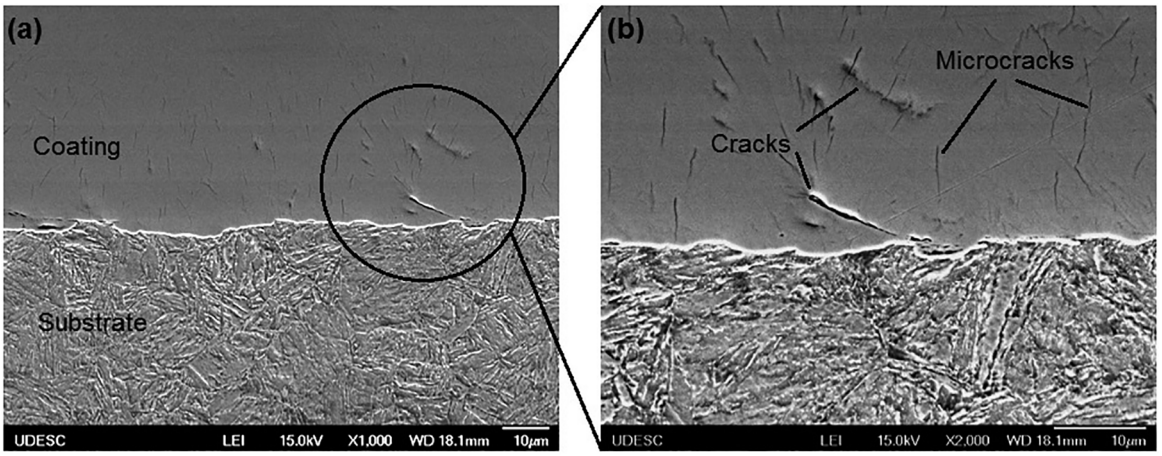

Figure 3. SEM images (secondary electrons) of hard chromium coated specimens. (a) coating overview and (b) detail of the black circle in (a)

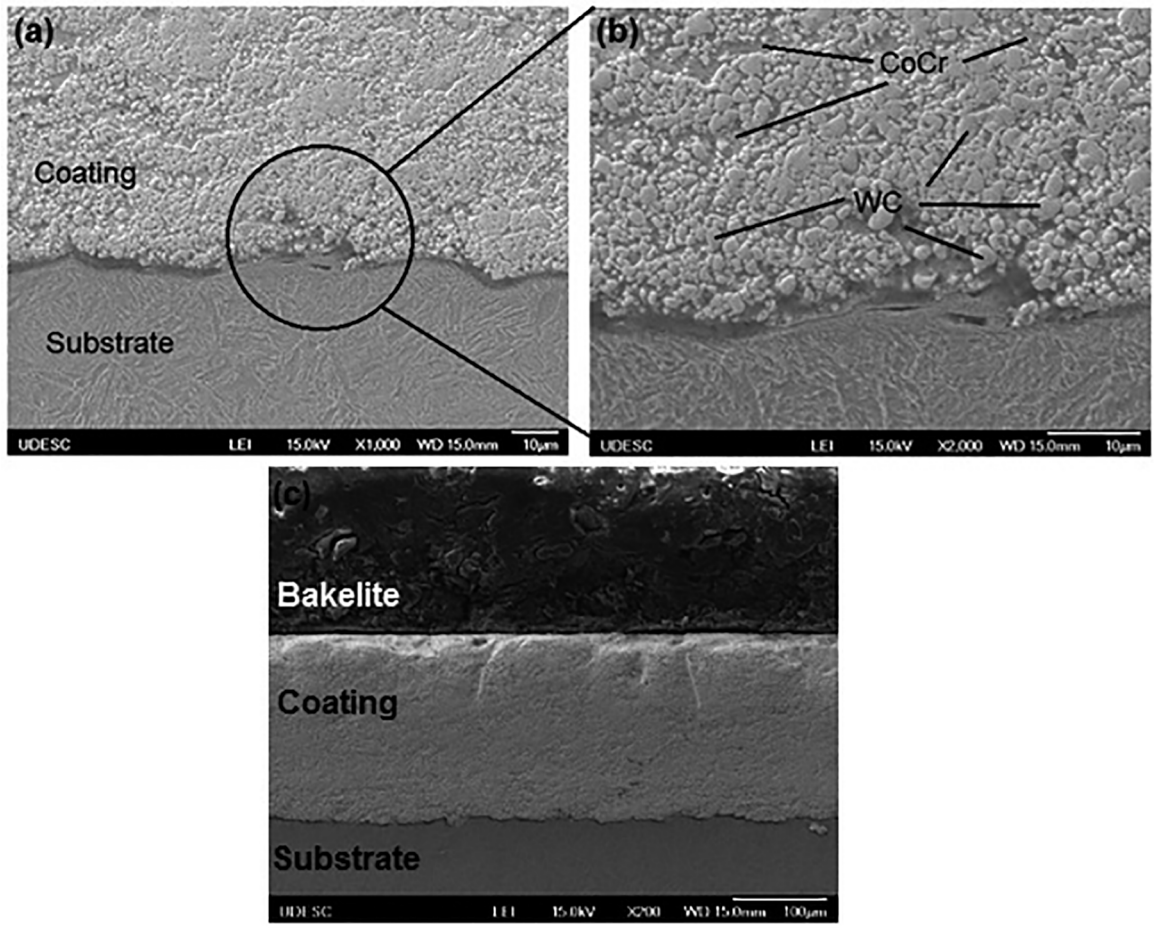

Figure 4. (a) coating overview, (b) detail of the black circle in (a) and (c) coating overview at lower magnification.

The microhardness profile of each specimen condition is shown in Figure 6. The coating-substrate interface region, after the grinding process (before wear tests), was achieved between 125 µm and 150 µm. The coating layers thickness obtained after the grinding process were 135 µm and 138 µm for hard chromium and WC-10Co-4Cr coatings, respectively.

The slight increase in hardness of the WC-10Co-4Cr coating near the coating-substrate region can be justified by the high speed and temperature of the powder particles at the time of contact with the substrate. When they collide with the surface of the base material, the coating particles are hot deformed which results in a noticeable increase in

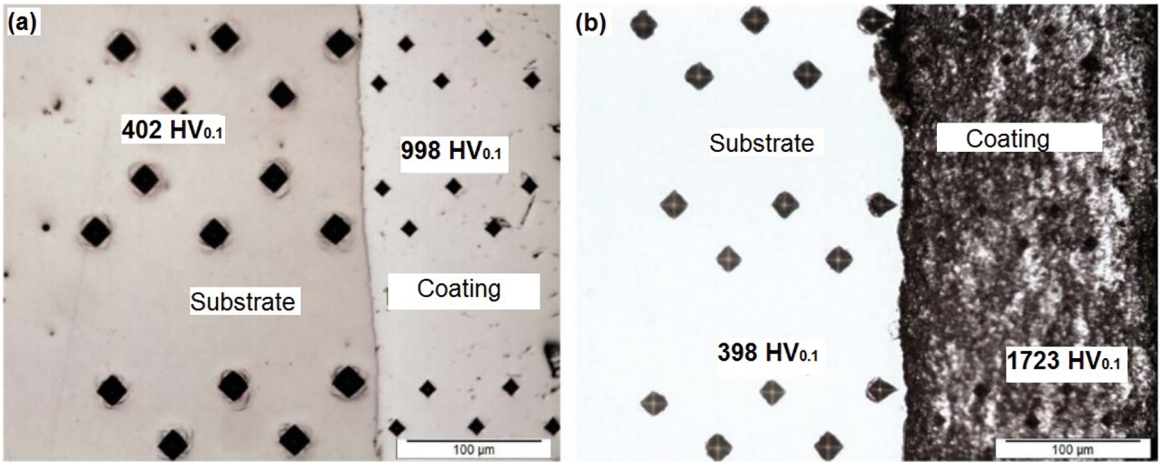

Figure 5. Vickers indentations ($HV_{0.1}$) in (a) hard chromium and (b) WC-10Co-4Cr coatings.

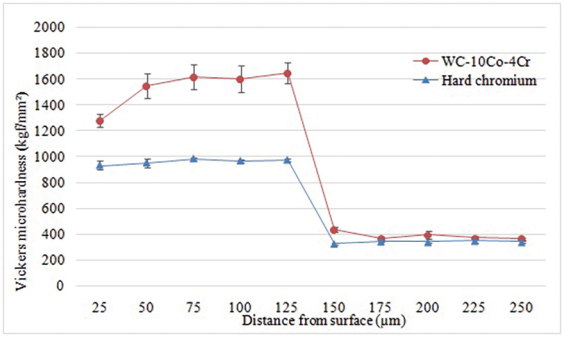

Figure 6. Microhardness profiles.

hardness of both the thermal HVOF sprayed coating and the substrate itself[8,29].

The microhardness values obtained were 1602 ± 42 kgf/mm² and 959 ± 20 kgf/mm² for WC-10Co-4Cr and hard chromium, respectively. The average hardness of the substrate was 363 ± 32 kgf/mm².

The higher dispersion of the microhardness values obtained for the thermally sprayed coating (WC-10Co-4Cr) are due to the heterogeneity of the HVOF sprayed coating since each point of the indentation may be located in different phases, in this case, carbides, oxides, inclusions and the matrix itself[30,31]. A dispersion of results is frequent since the characteristics of the spraying process lead to coatings with a certain degree of pores, oxides and unmelted grains which have different hardness values[32].

Even with the dehydrogenation treatment the chromium layer reached a high hardness. Since H+ ions are reduced at the cathode, together with Cr_6+ and Cr_3+, hydrogen in atomic form is dissolved by the chromium coating making it harder and therefore with less plasticity. Dehydrogenation partially decreases the hardness of the coating because it promotes the release of atomic hydrogen[2]. This factor may have been decisive so that the chromium coating did not reach even higher hardness values.

Quenched and tempered specimens achieved a hardness of 375 ± 25 kgf/mm² throughout the cross-section.

In comparative studies to replace the hard chromium coatings, the HVOF thermal spraying has shown excellent results related to the hardness of the coating. For the AISI 4340 steel the maximum hardness at the substrate-coating interface applied by HVOF showed to be superior to those with electroplated chromium coating due to the fact that the particles of the HVOF coating "explode" next to the surface of the substrate and achieve a greater adhesion and homogeneity of coating[8]. Similar result was also verified for low carbon steels substrates. In these materials, coatings of WC-12Co applied by HVOF reached hardness four times higher than hard chromium deposited by electrochemical treatment[33].

3.2. Tribological behavior

The volume of material removed (VMR) is shown in Figure 7. The best result was found to WC-10Co-4Cr coating, which is approximately 500 times lower than quenched and tempered (Q&T) AISI 4140 steel. The values obtained for hard chromium had a high degree of dispersion, with a standard deviation higher than 60% of the calculated average value.

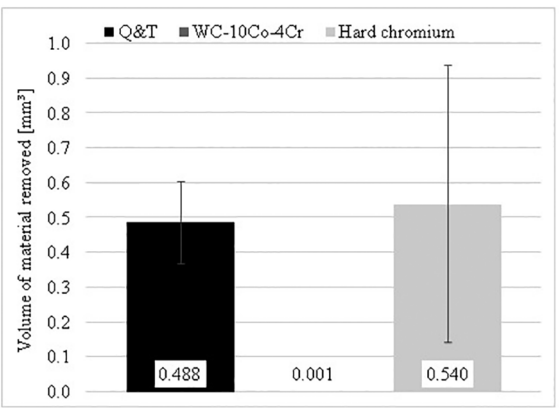

Figure 7. Volume of material removed (VMR).

The VMR values were $0.001 \pm 8.9x10^{-5}$ mm³ ($6.4x10^{-8} \pm 1.4x10^{-5}$ mm³/N.m) and $0.540 \pm 4.0x10^{-1}$ mm³ ($5.4x10^{-5} \pm 7.4x10^{-5}$ mm³/N.m) for WC-10Co-4Cr and hard chromium coatings, respectively. For Q&T condition the VMR was $0.488 \pm 1.2x10^{-1}$ mm³ ($4.9x10^{-5} \pm 2.4x10^{-5}$ mm³/N.m).

A high dispersion of results on pin-on-disc tests was verified. In the case of hard chromium, the dispersion may be related to the degree of hardness and the hydrogen content of the coating. A high hardness of the chromium layer can lead to more severe wear, because fragments of alumina (counter's-body material used), together with chromium particles, form brittle and cracked films that contribute to the continuous removal of material and coating spalling. The dehydrogenation of the chromium layer significantly increases the plasticity of the coating and contributes to the formation of a more wear resistant film for this tribo-system[2].

The presence of cracks inside the microstructure of the coating is another factor that can contribute to the variation of the results. Since they are random and depend on the electrodeposition process, some samples may have more cracks than others. During the cyclic loading caused in the pin-on-disc sliding test new cracks are formed which can be added to those existing in the material causing the spalling and the fragmentation of the chromium layer. This is a major disadvantage of this type of coating as it becomes more difficult to predict the performance of the coated materials by this method.

On the other hand, the HVOF (WC-10Co-4Cr) sprayed coating achieved excellent wear resistance performance. The combination of high temperature and velocity of the coating particles facilitates surface agglomeration and deformation[22]. Furthermore, small-sized powder particles, such as those used in this work, have aided the distribution and densification of the coating[28]. As a consequence, a compact solidification of the splats was obtained, promoting the filling of the pores and defects generated by the deposition of the first sprayed layers, as observed in the microstructural analysis of the coating (see Figure 4c). All these factors, coupled with the high hardness of the WC and W_2C particles contained in the coating (identified in the X-ray diffraction analysis) provided the excellent results of wear resistance with low amount of material removed, which is characteristic of this type of coating.

The wear track of Q&T AISI 4140 steel is shown in Figure 8. The white arrow in Figure 8a indicates the sliding direction. Figure 8b and 8c are higher magnifications of the dashed circles 1 and 2 (see Figure 8a), respectively.

The black arrows in Figure 8a indicate the formation of grooves/risks in the sliding direction. These grooves/risks are characteristics of abrasive wear mechanism and may have been caused by the plastic deformation of the substrate in contact with the counter-body or by the abrasion of wear debris that acted as abrasives during sliding[34]. The relatively low hardness of the uncoated material, compared to the counter-body, may have been a determining factor for this behavior.

In Figure 8b the detail 1 indicates the plastic deformation of the substrate. It could also be noted the presence of the grinding marks outside the wear track.

Figure 8c shows the presence of a large adhered particle and the occurrence of a crack formation that could be caused by a deformation process by transfer particles adhered to the counter-body. In Figure 8d, there is a detachment of the adhered wear particle (detail 1).

The wear track of hard chromium coated samples is shown in Figure 9. The white arrow indicates the sliding direction.

Compared with Figure 8, a reduction of wear by the abrasion and adhesion mechanisms is noted. The formation of wear particles in the sheet-like form (details 1 and 2 of Figure 9a) suggests that spalling may have occurred process as one of the acting wear mechanisms by brittle delamination fracture[35]. With the removal of these sheets there is exposure of a new surface (dashed rectangles in Figure 9b), more irregular and unprotected by the tribolayer formed between fragments of alumina, oxides and adhered chromium particles (dark region of Figure 9c). Apparently, this tribolayer has a fragile nature, and due to the existence of imperfections in the wear surface, it is removed and the wear process restarts[2]. The propagation of the inherent microcracks formed in the hard chromium coating to release residual stress[3] (see Figure 3) contributes to the formation of wear particles in the form of thin sheets.

Finally, the wear track of WC-10Co-4Cr coated samples is shown in Figure 10. The white arrow (see Figure 10a) indicates the sliding direction and the black arrow indicates the direction of the grinding marks. The detail 1 in Figure 10a is shown in Figure 10b and the detail 3 in Figure 10c is shown in Figure 10d.

Through Figure 10a it is possible to observe the permanence of the grinding marks inside the wear track, which proves the low volume of material removed during the sliding test. Small regions, such as those shown in Figures 10b-c, have more prominent wear marks. In these areas, it can be noticed that the most noticeable wear mechanism was also the spalling of the surface[11], however with a lower severity than that observed in the hard chromium layer of Figure 9. The compressive residual stresses promoted by the grinding process[18] retains the creation and propagation of the cracks, especially in HVOF-coated samples[17]. It is also noticeable the presence of small risks/grooves in the sliding direction, which indicates the occurrence of abrasive wear. This type of wear could be caused by high-hardness abrasive wear particles[13], as indicated by the black arrow in Figure 10d.

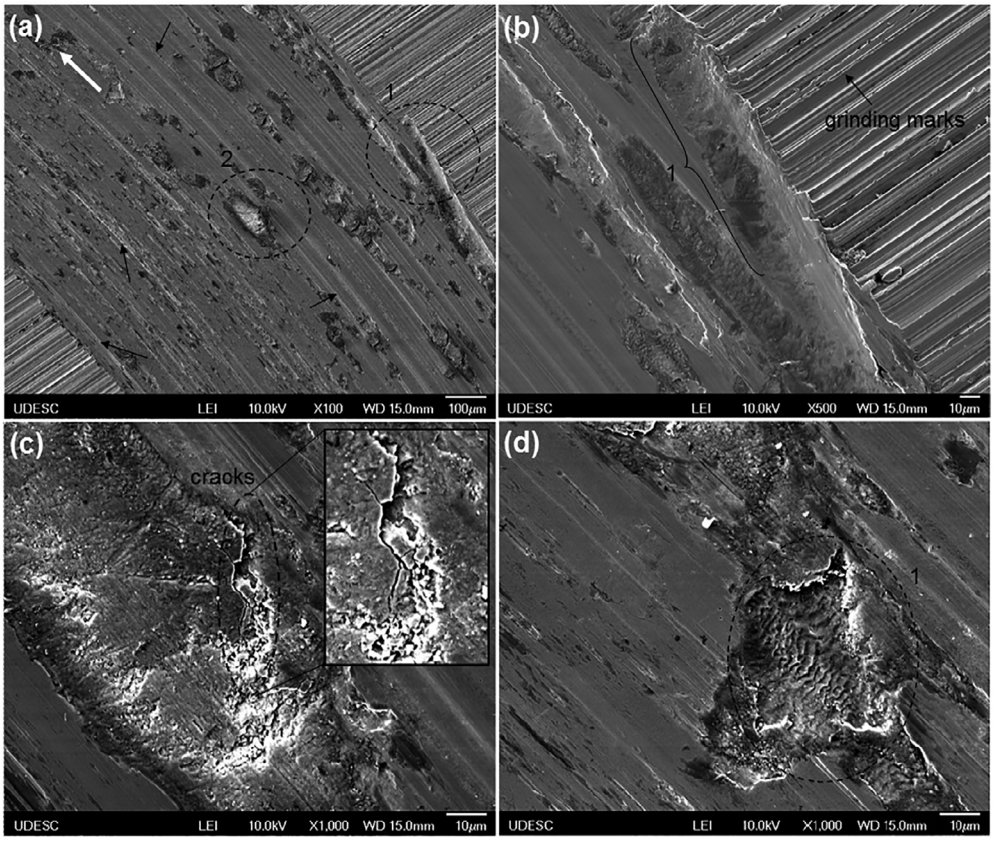

Figure 8. SEM images (secondary electrons) of the wear track of Q&T AISI 4140 steel samples.

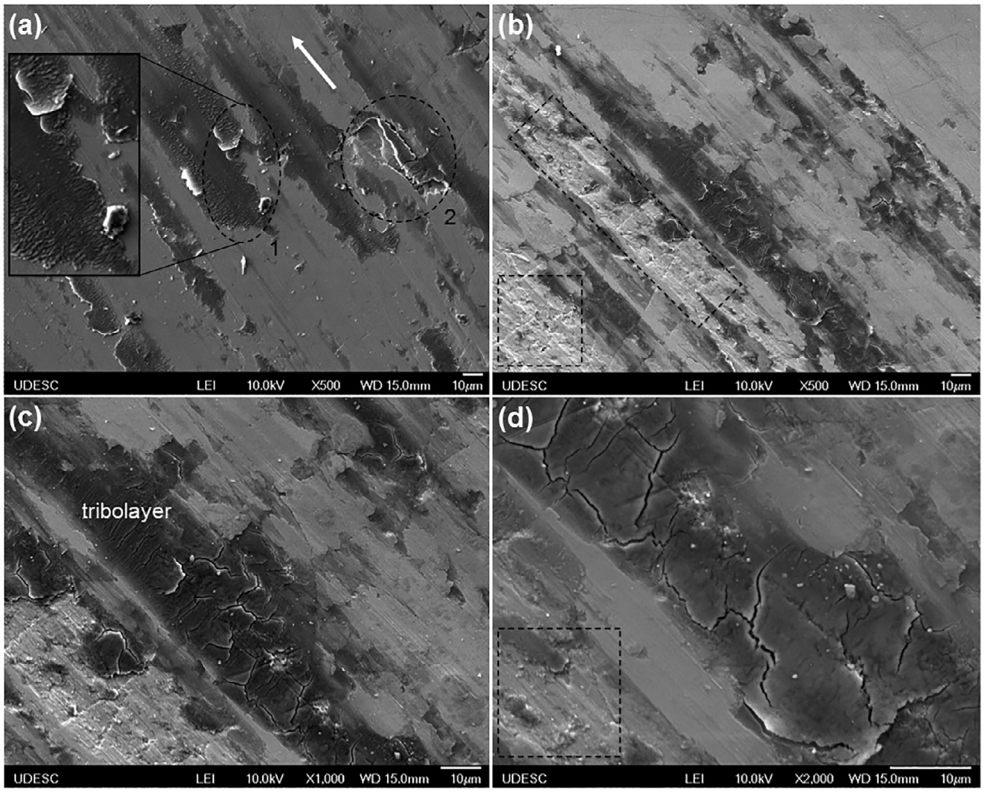

Figure 9. SEM images (secondary electrons) of the wear track of hard chromium coated AISI 4140 steel samples.

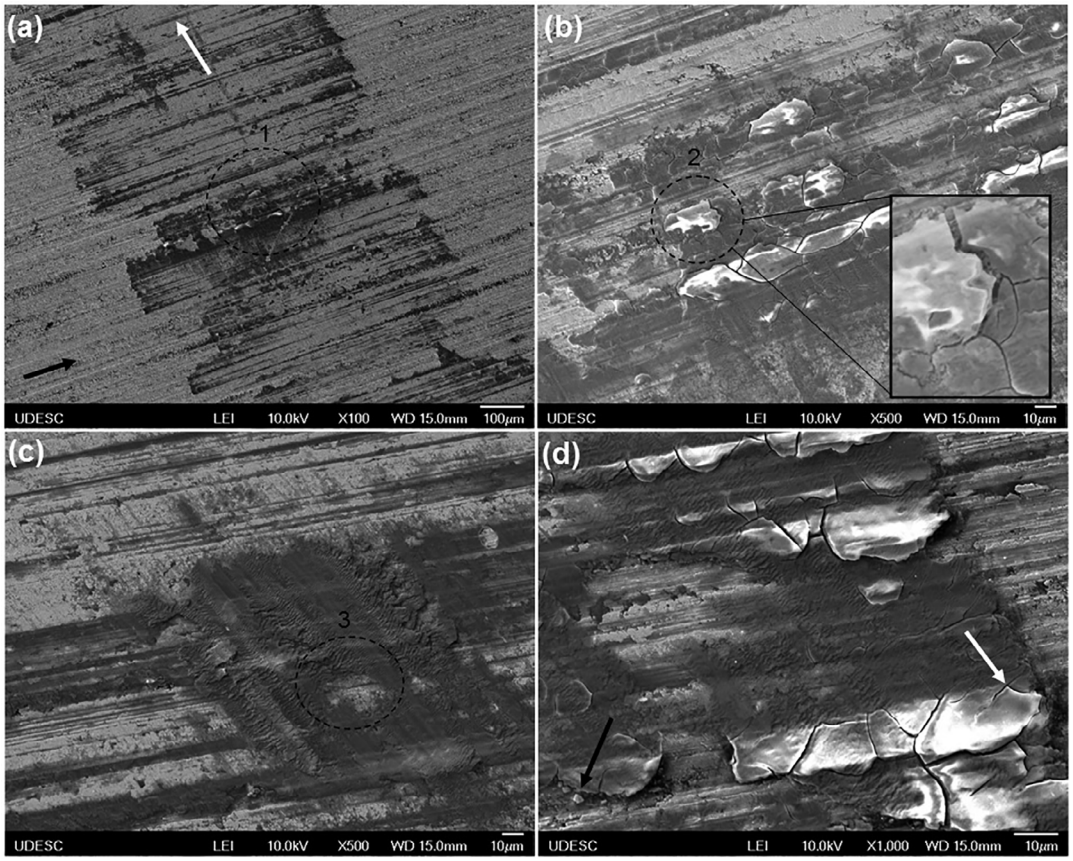

Figure 10. SEM images (secondary electrons) of the wear track of WC-10Co-4Cr coated AISI 4140 steel samples.

This behavior can be explained by the hardness contrast between the matrix and the tungsten carbide particles. When the harder phases (WC, W_2C) are pressed against a ductile matrix (CoCr) during the sliding contact, deformations occur in the matrix (white arrow indicated in Figure 10d) and embrittlement of the harder particles takes place. In this process, the matrix is extruded out of the surface of the coating by the compression of abrasive particles and little deformation capacity of the harder phases[36]. With the continuity of this event, there is the pull out of carbide phases due to extrusion of Co phase from the coating[17].

The tribolayer process formation on a wear surface is associated with the presence of a binding element that adheres to this adjacent surface[37]. Part of the extruded matrix may have been adhered to the counter body and to the small imperfections (pores and cracks) of the wear surface[36]. In contrast, abrasive micro-particles may bond together again through this adhered matrix and initiate the process formation of a tribolayer[24,38]. In this dense and well compacted new layer[19], cobalt acts by promoting the cohesion of the hard particles and fixing the film to the wear surface. The formed tribolayer protects the surface against new damages, reducing the wear rate to a lower value than the initial one[36].

4. Conclusions

The wear behavior of AISI 4140 steel coated by HVOF-, EHC-process and Q&T steel was investigated. Samples were grinded prior to sliding tests to achieve surface roughness to about 1 μm. Based on the experimental results it is possible to formulate the following conclusions:

- The wear resistance of the WC-10Co-4Cr HVOF-sprayed coating was found to be about 500 times greater than the wear resistance of the SAE 4140 steel Q&T condition. For hard chromium coating the wear resistance was 2 times greater than achieved to Q&T condition;
- Adhesion and abrasion due to plastic deformation were the main wear mechanisms observed in Q&T samples;
- The delamination of a tribolayer of fragile nature added to a microstructure with high density of cracks are factors that may have led to a more pronounced wear of the hard chromium coated samples;
- The high hardness associated with the formation of a wear resistant tribolayer were determinants to the excellent wear behavior of WC-10Co-4Cr HVOF-sprayed coating.

5. References

1. Houdková Š, Zahálka F, Kašparová M, Berger LM. Comparative Study of Thermally Sprayed Coatings Under Different Types of Wear Conditions for Hard Chromium Replacement. *Tribology Letters*. 2011;43(2):139-154.

2. Bolelli G, Cannillo V, Lusvarghi L, Riccò S. Mechanical and tribological properties of electrolytic hard chrome and HVOF-sprayed coatings. *Surface and Coatings Technology*. 2006;200(9):2995-3009.

3. Almotairi A, Warkentin A, Farhat Z. Mechanical damage of hard chromium coatings on 416 stainless steel. *Engineering Failure Analysis*. 2016;66:130-140.

4. Ibrahim A, Berndt CC. Fatigue and deformation of HVOF sprayed WC-Co coatings and hard chrome plating. *Materials Science and Engineering: A*. 2007;456(1-2):114-119.

5. Liang A, Li Y, Liang H, Ni L, Zhang J. A favorable chromium coating electrodeposited from Cr(III) electrolyte reveals anti-wear performance similar to conventional hard chromium. *Materials Letters*. 2017;189:221-224.

6. Brooman EW. Wear behavior of environmentally acceptable alternatives to chromium coatings: cobalt-based and other coatings. *Metal Finishing*. 2004;102(10):42-54.

7. Legg KO. Hard chromium replacements. In: *4th International Chromium Conference*; 2004 May; St. Etienne, France.

8. Souza RC, Voorwald HJC, Cioffi MOH. Fatigue strength of HVOF sprayed Cr_3C_2-25NiCr and WC-10Ni on AISI 4340 steel. *Surface and Coatings Technology*. 2008;203(3-4):191-198.

9. Voorwald HJC, Padilha R, Costa MYP, Pigatin WL, Cioffi MOH. Effect of electroless nickel interlayer on the fatigue strength of chromium electroplated AISI 4340 steel. *International Journal of Fatigue*. 2007;29(4):695-704.

10. Picas JA, Punset M, Baile MT, Martín E, Forn A. Tribological evaluation of HVOF thermal-spray coatings as a hard chrome replacement. *Surface and Interface Analysis*. 2011;43(10):1346-1353.

11. Gong T, Yao P, Zuo X, Zhang Z, Xiao Y, Zhao L, et al. Influence of WC carbide particle size on the microstructure and abrasive wear behavior of WC-10Co-4Cr coatings for aircraft landing gear. *Wear*. 2016;362-363:135-145.

12. Singh J, Kumar S, Mohapatra SK. Tribological analysis of WC-10Co-4Cr and Ni-20Cr_2O_3 coating on stainless steel 304. *Wear*. 2017;376-377(Pt B):1105-1111.

13. Bolelli G, Berger L, Bonetti M, Lusvarghi L. Comparative study of the dry sliding wear behaviour of HVOF-sprayed WC-$(W,Cr)_2C$-Ni and WC-CoCr hardmetal coatings. *Wear*. 2014;309(1-2):96-111.

14. Hong S, Wu Y, Wang B, Zheng Y, Gao W, Li G. High-velocity oxygen-fuel spray parameter optimization of nanostructured WC-10Co-4Cr coatings and sliding wear behavior of the optimized coating. *Materials & Design*. 2014;55:286-291.

15. Wu Y, Wang B, Hong S, Zhang J, Qin Y, Li G. Dry Sliding Wear Properties of HVOF Sprayed WC-10Co-4Cr Coating. *Transactions of the Indian Institute of Metals*. 2015;68(4):581-586.

16. Wu D, Liu Y, Li D, Zhao X, Liu Y. Tribo-corrosion properties of WC-10Co-4Cr coating in natural silt-laden waters when sliding against Si3N4. *International Journal of Refractory Metals and Hard Materials*. 2016;58:143-151.

17. Zoei MS, Sadeghi MH, Salehi M. Effect of grinding parameters on the wear resistance and residual stress of HVOF-deposited WC-10Co-4Cr coating. *Surface and Coatings Technology*. 2016;307(Pt A):886-891.

18. Murthy JKN, Rao DS, Venkataraman B. Effect of grinding on the erosion behaviour of a WC-Co-Cr coating deposited by HVOF and detonation gun spray processes. *Wear*. 2001;249(7):592-600.

19. Federici M, Menapace C, Moscatelli A, Gialanella S, Straffelini G. Pin-on-disc study of a friction material dry sliding against HVOF coated discs at room temperature and 300 °C. *Tribology International*. 2017;115:89-99.

20. Gadelmawla ES, Koura MM, Maksoud TMA, Elewa IM, Soliman HH. Roughness parameters. *Journal of Materials Processing Technology*. 2002;123(1):133-145.

21. Guilemany JM, Espallargas N, Suegama PH, Benedetti AV. Comparative study of Cr_3C_2-NiCr coatings obtained by HVOF and hard chromium coatings. *Corrosion Science*. 2006;48(10):2998-3013.

22. Kang AS, Grewal JS, Cheema GS. Effect of thermal spray coatings on wear behavior of high tensile steel applicable for tiller blades. *Materials Today Proceedings*. 2017;4(2 Pt A):95-103.

23. Picas JA, Punset M, Baile MT, Martín E, Forn A. Properties of WC-CoCr Based Coatings Deposited by Different HVOF Thermal Spray Processes. *Plasma Processes and Polymers*. 2009;6(Suppl 1):S948-S953.

24. Schwetzke R, Kreye H. Microstructure and properties of tungsten carbide coatings sprayed with various high-velocity oxygen fuel spray systems. *Journal of Thermal Spray Technology*. 1999;8(3):433-439.

25. Bozzi AC, De Mello JDB. Wear resistance and wear mechanisms of WC-12%Co thermal sprayed coatings in three-body abrasion. *Wear*. 1999;233-235:575-587.

26. Kear BH, Skandan G, Sadangi RK. Factors controlling decarburization in HVOF sprayed nano-WC/Co hardcoatings. *Scripta Materialia*. 2001;44(8-9):1703-1707.

27. Sziráki L, Kuzmann E, Papp K, Chisholm CU, El-Sharif MR, Havancsák K. Electrochemical behaviour of amorphous electrodeposited chromium coatings. *Materials Chemistry and Physics*. 2012;133(2-3):1092-1100.

28. Wood RJK. Tribology of thermal sprayed WC-Co coatings. *International Journal of Refractory Metals and Hard Materials*. 2010;28(1):82-94. DOI: http://dx.doi.org/10.1016/j.ijrmhm.2009.07.011

29. Berger LM, Saaro S, Naumann T, Wiener M, Weihnacht V, Thiele S, et al. Microstructure and properties of HVOF-sprayed chromium alloyed WC-Co and WC-Ni coatings. *Surface and Coatings Technology*. 2008;202(18):4417-4421.

30. Lee CW, Han JH, Yoon J, Shin MC, Kwun SI. A study on powder mixing for high fracture toughness and wear resistance of WC-Co-Cr coatings sprayed by HVOF. *Surface and Coatings Technology*. 2010;204(14):2223-2229. DOI: http://dx.doi.org/10.1016/j.surfcoat.2009.12.014

31. Sidhu BS, Prakash S. Evaluation of the corrosion behaviour of plasma-sprayed Ni_3Al coatings on the steels in oxidation and molten salt environments at 900 °C. *Surface and Coatings Technology*. 2003;166(1):89-100.

32. Nucci R. *Avaliação da resistência ao desgaste de cermets depositados pelo processo de HVOF e do cromo duro eletrolítico*. [Dissertation]. São Carlos: Universidade de São Paulo; 2005. 97 p.

33. Castro RM. *Avaliação das propriedades de superfície e do comportamento ao desgaste abrasivo de hastes de cilíndros hidráulicos revestidas pelos processos HVOF e cromo duro eletrodepositado*. [Dissertation]. Porto Alegre: Universidade Federal do Rio Grande do Sul; 2012. 96 p.

34. Pawlowski L. *The Science and Engineering of Thermal Spray Coatings*. 2nd ed. Chichester: John Willey & Sons; 2008.

35. Hazra S, Sabiruddin K, Bandyopadhyay PP. Plasma and HVOF sprayed WC-Co coatings as hard chrome replacement solution. *Surface Engineering*. 2012;28(1):37-43.

36. Krelling AP, Milan JCG, da Costa CE. Tribological behaviour of borided H13 steel with different boriding agents. *Surface Engineering*. 2015;31(8):581-587.

37. Gunes I. Wear Behaviour of Plasma Paste Boronized of AISI 8620 Steel with Borax and B_2O_3 Paste Mixtures. *Journal of Materials Science & Technology*. 2013;29(7):662-668.

38. Yang Q, Senda T, Ohmori A. Effect of carbide grain size on microstructure and sliding wear behavior of HVOF-sprayed WC-12% Co coatings. *Wear*. 2003;254(1-2):23-34.

39. Blomberg A, Hogmark S, Lu J. An electron microscopy study of worn ceramic surfaces. *Tribology International*. 1993;26(6):369-381.

40. Vashishtha N, Khatirkar RK, Sapate SG. Tribological behaviour of HVOF sprayed WC-12Co, WC-10Co-4Cr and Cr_3C_2-25NiCr coatings. *Tribology International*. 2017;105:55-68.